

# Numerical Analysis of the Primer Location Effect on Ground Vibration Caused by Blasting

Moein Bahadori <sup>a</sup>, Hassan Bakhshandeh Amnieh <sup>b\*</sup>

<sup>a</sup> Department of Mining Engineering, University of Gonabad, Gonabad, Iran

<sup>b</sup> School of Mining, College of Engineering, University of Tehran, Tehran, Iran

## Article History:

Received 05 July 2016,

Revised 26 November 2016,

Accepted 28 November 2016.

## ABSTRACT

Ground vibration is one of the undesirable outcomes of blasting operations. Different methods have been proposed to predict and control ground vibration that is caused by blasting. These methods can be classified through laboratory studies, fieldwork and numerical modeling. Among these methods, numerical modeling is the one which takes into account the basic principles of mechanics and provides step by step time-domain solutions to save time and budget. In order to use numerical analysis in predicting the results of blasting operations, the accuracy of the output must be verified through field test. In this study, the ground vibration caused by blasting in a field operation in Miduk Copper Mine was recorded using 3-component seismometers of the Vibracord seismograph and analyzed by Vibration-Meter software. Propagation of the waves caused by blasting in the mine slope was modeled using discrete element logic in the UDEC numerical software and was compared to that of the field test. Having tested the accuracy of the results, the effect of primer location and the direction of detonation propagation in the blast hole on the rate of ground vibration caused by blasting was investigated. The results show that by changing primer location from the bottom of the hole to its top, the rate of ground vibration caused by blasting increases.

**Keywords :** *Blasting, Ground vibration, Numerical modeling, Primer, Vibracord seismograph, Miduk*

## 1. Introduction

Blasting is a very rapid physicochemical phenomenon and release a very high amounts of light, heat and pressure when it takes place [1-3]. Generally, the results of blasting operations include fly rock, ground and air vibration, back-break, fragmentation and movement of the fragmented pile. Prediction and control of these factors has an effective role in reducing total costs of mining operations. Sudden change in the distance among molecules from some angstroms in an unburned explosive to several millimeters in the gases produced by blasting creates shock waves that affect the rock adjacent to the blast hole [1-4]. The initial energy released by blasting is so high that turns a certain part of the blast-hole wall into powder. Increasing the distance from charge (hole) center and attenuation due to severe deformation creates another zone of plastic deformations around the blast hole which is called the cracked zone. These cracks develop with the leakage of gases produced by blasting [1, 2, and 5]. Due to severe attenuation caused by plastic deformation in the first two areas, blasting energy appears only in the form of vibrating waves outside the domain of radial cracks that can damage the environment around the structures. Singh & Singh (2005) showed that only 20 to 30 percent of the energy caused by blasting is spent on the fragmentation of the rock mass and the rest takes the forms of fly-rock, ground and air vibration, back-break and movement of the fragmented pile. Prediction and control of such variables can reduce the total costs of mining operations to a large extent [6]. The results of blasting operations can be controlled by the mutual effects of rock properties (in-situ stresses, joints, pre-existing micro-fractures, rock strength and bedding plans), explosives (velocity of detonation, density,

detonation pressure and water resistance) and blasting pattern (blast direction, burden and spacing, hole depth and delay times) and true understanding of this concept depends on direct observation and experimentation [1, 2, 7, 8]. Therefore, researchers have tried to predict different results of blasting operations and to optimize such operations using numerical techniques [9-13], fieldwork and laboratory studies [14-25] as well as analytical investigations [26-28]. Although numerical modeling has some shortcomings and limitations, it has been applied more widely to predict and control the blasting results compared to other methods since it saves time and reduces costs. Advances in computer systems have also contributed to the widespread use of this method. Generally, numerical methods can go under three main categories for analyzing the results of blasting operations: pre-fracture models (DEM), continuous models with plastic deformation in elements (FEM) and modern hybrid models (HSBM, XFEM). In the first category, the process of blasting is modeled using discrete element logic (DEM, DDM and DDA) and the given area is fractured into certain dimensions before loading, and after the application of the dynamic loads, fractures develop along predetermined paths and turn the block into fragments. This method has the ability to analyze rigid or deformable blocks and provides the ground vibration analysis for deformable blocks. The first computer codes applied to analyze fragmented rock movement after blasting was prepared by Kirby et al. (1989) and Harris (1989) in Sandia National Laboratory with the brand name of SABREX. In these codes, it is assumed that the fragmented rock mass consists of blocks fractured in similar dimensions before blasting [29, 30]. Yang & Kavetsky (1998, 1990) introduced a computer code to estimate the potential pile movement by different explosives and to control dilution. The results of these studies show that by increasing the

\* Corresponding author. Tel.: (+98)21 61114141. E-mail address: [hbakhshandeh@ut.ac.ir](mailto:hbakhshandeh@ut.ac.ir) (H. Bakhshandeh).

delay time among the rows or reducing the hole's angle from a vertical position, geometric expansion of the pile would be larger [31, 32]. For blast numerical modeling, Preece and Knudsen (1992) from Sandia National Laboratory proposed various two-dimensional models of the fragmented pile movement caused by the expansion of gases produced by blasting called DMC [33]. Preece (1992) investigated the effect of pile geometry on loading costs and modeled slight (less than 50 ms) delay times to high (more than 300ms) delay times among the rows. According to the results of this investigation, the cast percent is related to delay times [34]. Chung et al. (1994) compared the results of field blasting operations in opencast coal mines with that of DMC and SABREX computer models. They concluded that although there is good consistency between the results of such modeling and the values recorded in fieldwork, DMC code is able to model more complex situations than the SABREX code [35]. The studies conducted by Chen and Zhao (1998) can be generally divided into three categories: numerical modeling of blasting in a continuous medium (in Autodyn2D software), numerical modeling of blasting in a discontinuous environment (in UDEC software) in the presence of a single discontinuity at different intervals from the blasting post and in the presence of two groups of discontinuities with different hardness. According to these studies, for continuous conditions and with similar loading, numerical modeling renders the same responses using the two types of software [36]. Preece and Chung (1999) considered the ability to analyze strength properties of coal into the DMC code in order to reduce damage to the layers of surface coal and used cast blasting in their numerical analysis. The results of this study show that a thin area in the upper part of the coal layer adjacent to the fragmented overburden is damaged, and on the free-face, part of the coal layer is fragmented through a cut-like process and is separated from the layer [37]. Chen et al. (2000) studied blasting waves' damping as a result of hitting the internal surfaces of discontinuity in a fractured rock mass using numerical analysis in the UDEC discrete element software. The results of their numerical analysis indicate that in a state of non-linear behavior, wave transient coefficient depends on wave length when the wave moves away from discontinuity, while in a state of linear behavior there is no relationship between the two parameters [9]. To study the effects of burden and discontinuities on the fragmented rock's movement, Mortazavi and Katsabanis (2001) used an implicit solution technique called DDA [38]. This method was first introduced by Shi (1992) [39]. Firth and Taylor (2001) used discrete element logic in the UDEC software and modeled the blasting process in a hole to study the ore grade distribution. The results of their numerical analysis show how grade distribution in the fragmented pile takes place after the final movement, and also the low-grade section which is often adjacent to the collar, has no significant horizontal movement and can be easily separated from the ore [40]. Fan et al. (2004) used UDEC discrete element software to investigate the effect of exercising dynamic loading in the form of Velocity History Input (VHI) or Stress History Input (SHI). The results of their numerical analysis showed that unlike velocity boundary conditions, in dynamic loading that uses stress boundary conditions, the boundary under loading is not completely constrained and can move. Therefore, with respect to the possibility of discontinuity opening, wave damping increases under stress boundary conditions [41]. Kim et al. (2007) applied PFC2D software to model blasting in the tunnel's cross-section using deep holes method. According to the results of the field experiment carried out by Kim et al. (2004), under similar conditions, the rate of vibrations caused by blasting using SAV-cut method is reduced by 10% compared to the wedge method [11]. In their rock fragmentation modeling of a road tunnel, Yoon and Jeon (2010) used PFC2D software to control damages caused by blasting in buffer holes. The results of numerical analysis showed that in controlled blasting operations in buffer holes, using explosives with less explosion pressure, the radius of the powdered zone around the blast hole can be reduced without decrease in the length of the radius cracks [12]. Ning et al. (2011) used two-dimensional DDA method in their estimation of the muck-pile geometry after blasting [42]. Aliabadian et al. (2014) used UDEC discrete element software to investigate the effect of distance and orientation of a unique

discontinuity on wave propagation and the cracks caused by blasting. The results of this study showed that in comparison to shear components, horizontal and vertical stress components have a higher share in cracks growth. Besides, the researchers examined the cause of cracks growth in certain paths and concluded that the main reason was the higher residual stress in deformed elements after the passage of wave front [43]. Sharafisafa et al. (2014) modeled the results of pre-fractured blasting operations using UDEC discrete element software and concluded that the spread of plastic deformation in a set of adjacent elements is equivalent to the development of plastic zones. The results of this study showed that exercising pre-fractured blasting operations using an explosive with the density of 1.45 kg/m<sup>3</sup> and the detonation velocity of 3000 m/s is optimal when the explosive and the hole are coupled and the spacing among blast holes is within the range of 0.5m to 1m. Numerical analyses, on the other hand, show that selecting values greater than this spacing (between 2m to 4m) increases undesirable crack growth and the spacing of up to 4m does not allow the cracks to meet along the pre-fracture line [44]. Yan et al. (2016) investigated the effects of blasting pattern parameters such as burden length and slope height on pile movement using 3DEC. In this study, in order to accelerate the calculations, the crushed zone around the blast hole was neglected. Moreover, to model the rock fragmentation and pile movement, the area was split to a uniform distribution of cubic blocks, using three perpendicular same-spacing artificial joint-sets. As Yan et al. (2016) stated, it is expected that increasing the slope height and decreasing the burden length cause more geometrical spread in the pile of fragmented rocks. This is while the results of numerical models showed that the geometric spread of fragmented material has a direct relation with both parameters. Finally, these researchers concluded that the factors affecting the geometrical shape of the pile were including: burden length, intensity of fragmentation and bench height, in order of importance [45]. Bahadori et al. (2016) proposed a new geometrical-statistical algorithm to model the rock fragmentation by blasting. In their study, using image analysis technique, the fragmentation distribution of a special field test of rock blasting was measured. Then the ability of four statistical algorithms to accurately predict size distribution of fragmented material was compared. The investigated algorithms were the orthogonal, random oriented and Voronoi algorithms, and they also proposed a separate algorithm. The results showed that the proposed algorithm kept the mean value of the fragmented material in a variety of uniformities. Since the proposed algorithm could model the roughness and wavy properties of discontinuities surface, Bahadori et al. (2016) suggested that it could be implemented in DEM numerical modeling of rock fragmentation, fluid flow analysis, and slope stability analysis [46].

The second category of studies includes analyses of homogenous and continuous medium where modeling fractures and crack spread is conducted with respect to the deformation of elements. Starfield and Pugliese (1974) used the finite element method in the validation of computer models with field measurements carried out after the explosion of cylindrical charges [47]. Preece and Thorne (1996) used the finite element technique in the PRONTO<sup>3D</sup> code in order to evaluate the effect of delay times on rock fragmentation caused by dynamic loading [48]. Liu and Katsabanis (1997) used the Abaqus finite element software in studying delay times at two ends of a hole when blasting starts. They also studied the effect of the superposition of the waves caused by two wave fronts on fragmentation caused by blasting. According to this study, simultaneous detonation of the charge at two ends of a hole results in constructive waves superposition in the middle of the blast hole and fragmentation intensification in this part [49]. Wenxue et al. (2002) simulated the dynamic damage effects caused by blasting in sandstone using JWL equation of state in the LS-DYANA<sup>3D</sup> finite element software [50]. Cho et al. (2003) introduced a numerical modeling method based on finite element logic in order to study the effect of pattern dimension on size distribution of the fragmented material caused by blasting in numerical and image analysis techniques. According to the results of numerical modeling, radial cracks develop around the blast hole and only outside the fragmented zone, and the reflection of pressure waves in tensile form on the free surface will lead

to the development of more tensile fractures and the swelling of the rock pile on the free surface [51]. Jha et al. (2010) used LS-DYNA finite element software in their numerical simulation of investigating the effect of blasting in an open-pit mine on an adjacent underground mine. In this study, the ground vibration caused by 73 blasting operations in the roof, floor and wall of the underground mine were recorded and compared to the results of numerical modeling [52]. To accurately estimate the fragmentation process around the blast hole, the force transferred to the burden, the increase in the hole volume, and the movement of gaseous products of blasting to stemming and into the cracks around the hole, Sellers (2012) proposed a pressure-time model and compared its results to the results of field experiments and other numerical models. According to the values recorded in the numerical modeling, Sellers (2012) believes that the potential energy of blasting gases at 10 $\mu$ s after explosion reaches its peak, and due to severe plastic deformations around the blast hole, a significant part of the hole dilation work is lost at 100 $\mu$ s and the rest of the energy passes in form of strain energy and creates ground vibrations [13]. Sazid and Singh (2013) used the Abaqus finite element software in their two-dimensional modeling of blasting. Based on their numerical modeling, since the velocity of detonation was assumed to be between 2500m/s and 6000m/s, the strain energy caused by blasting was within the range of 12.89kj to 51.99kj, respectively [53].

In hybrid methods, continuous and discontinuous methods are combined with the aim of omitting the undesirable properties of each method and optimizing the use of their desirable characteristics in modeling the problems. The main combinations are BEM/FEM, DEM/FEM and DEM/BEM [54]. Since 2001, an international project has been carried out by Queensland University in Australia, Cambridge and Leeds universities in the United Kingdom and the ITASCA group of consultants to provide a detailed numerical modeling method with the ability to simulate the blast loading, fracturing and fragmentation processes in a rock mass and the eventual pile movement. This project is called "Hybrid Stress Blasting Model (HSBM)" and uses hybrid computations of continuous and discontinuous calculation logics in evaluating the results of rock fragmentation by blasting. The computational logic used in HSBM, is an adaptation of DMC calculation method. In HSBM, using three different computational logics, the blasting process is modeled in three separate ranges including the explosive material column, the powdered zone (2.5 times larger than the radius of the hole) and the cracks caused by blasting. The PFC logic is used to model the fractured zone and thus the rock mass is broken down into pieces with a specified uniform size before blasting. These pieces are connected by the Kelvin-Voigt equation (parallel spring and damper) and tensile strength. In this model, the estimated fragmentation intensity, depends on the network size and since all the fractured area (outside the powdered region) is modeled using this

network, reducing network size will considerably increase the time and number of calculations [55]. To validate the results of numerical analysis through blasting experiments in the field, Onederra et al. (2010) used a network of discrete elements instead of PFC<sup>3D</sup> logic. According to the results of field blasting experiments, estimation of the average size for fragments created by blasting using numerical modeling in Blo-Up software in cubic and cylindrical models has 23% and 11% error rates, respectively [56]. Sellers et al. (2010) applied HSBM model in estimating the results of large-scale field experiments. Although the results of numerical modeling through HSBM shows acceptable estimations of changes in velocity and acceleration of particles, this model is weak in determining extreme values [57]. To validate predictions carried out using HSBM, Sellers et al. (2012) compared the results of field blasting experiments with the numerical analyses of HSBM [58]. In modeling large-scale blasts, Sellers et al. (2012) studied the results of two models with 15 and 60 blast holes using HSBM. Assuming there was a constant ratio between the burden and the lateral spacing of the blast holes (hole diameter of 165mm), as the specific charge decreases (or the burden and spacing increases), the pile geometry increases and the surface spread decreases.

In this study, a field blasting experiment was conducted to validate the results of numerical modeling including ground vibration, fragmentation, back-break and movement of the fragmented rock. Using the UDEC discrete element software, we modeled the blasting operation and assessed the accuracy of its results in estimation of ground vibration rate caused by blasting. Finally, based on the results obtained in numerical modeling, the effect of the primer location on the rate of ground vibration caused by blasting was investigated in numerical and analytical terms.

## 2. Methodology

### 2.1. General Geology of Miduk Copper Mine

Miduk copper mine is located 42 km northeast of Shahrabak and 132 km northwest of Sarcheshmeh copper mine in Kerman province in longitude and latitude of 55 10' and 30 25', respectively. The main mine pit is located 7 km northwest of Miduk village. Fig. 1 shows the geographical location and access ways to Miduk copper mine. The total known geological volume of the ore body is estimated about 180 MT with an average grade of 0.83 from which only a reservoir of 144 MT is minable. From a geological perspective, the ore body is hosted by an intrusive Monzonite suite. The cutoff grade, W/O, slope height, berm width, and final pit angle are calculated to be 0.25, 2.4, 15m, 9m, and 38°, respectively. The annual productivity is programmed to be 5MT and the mine lifespan is estimated to be 29 years.

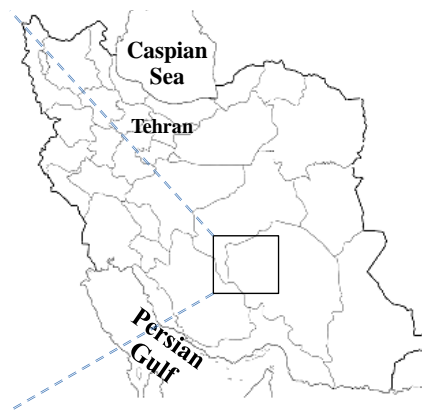
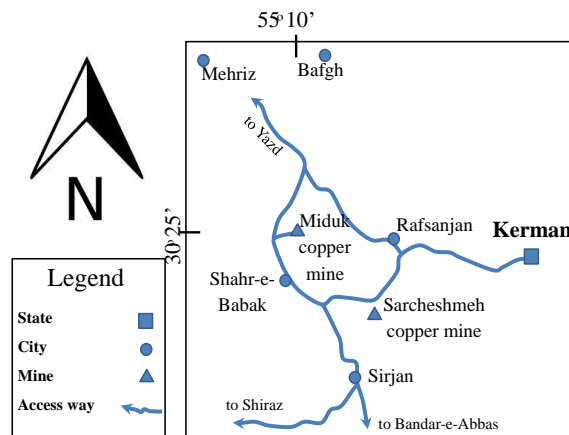


Fig. 1. Geographical location and access roads to Miduk Copper Mine.

### 2.2. Excavation and blasting in Miduk Copper Mine

The slopes were designed with the height and width of 15m and 20m, respectively. Depending on geological conditions, the blast holes are drilled with the diameter of 6in to 8in, the depth of 17m (considering 2m of sub-drilling) in 5m×6.5m, 5.5m×7m, and 6.5m×8m staggered patterns, using 12 TEREX, Ingersoll Rand, and T4 drilling machines. The main charge used is ANFO and Emulan for dry and wet holes, respectively. The initiation system is always non-electric (NONEL and/or Cortex) with the delay timing of 25, 42, 50, and 65ms in diurnal blasting operations. On average, one blasting operation is conducted every day. Mechanical and physical properties of the Quartzite rock masses of Miduk copper mine are presented in Table 1.

Table 1. Physical and mechanical properties of Quartzite rock masses used in numerical analysis.

Row	Property	Unit	Phyllic	Quartzite
1	Density	kg/m <sup>3</sup>	2370	2650
2	Uniaxial compressive stress	MPa	40	93
3	Tensile strength	MPa	3.5	4.5
4	Cohesion	MPa	4.3	6.2
5	Internal friction angle	°	32	29
6	Elastic modulus	GPa	65	130
7	Poisson's ratio	-	0.23	0.21

### 2.3. Field blasting experiment

To verify the accuracy and precision of the estimation about fragments size distribution, a rock blasting experiment was carried out in the quartzite rock mass using geometric algorithms. The measured field data are including geological conditions, water head inside blast holes, discontinuities, initial and final geometry of the blocks, the blast pattern, fragmentation, back break, and pile movement. Fig. 2 shows the blasting block in a topographic map, seismograph location, the detonation time of each blast hole and the geometrical situation of the selected area for the field test. Fig. 3 shows the collar of the blast hole and the initial geometry of the block before blasting. The data from exploratory boreholes showed that RQD of the rock mass in the range

of the blasting block was almost 50 and the measurements showed that the area was completely dry. As seen in Figure 3, the aggregation of discontinuities in the area caused domain instability and some partial downfalls in the crest. The stemming length was about 7m and the burden and spacing lengths were 6.5m and 8m, respectively. The main charge was ANFO, and the inter-hole and in-hole delay times were 65ms and 42ms, respectively. The 500ms detonator was used to initiate the 3 pounds booster (primer) at the bottom of the holes.

### 2.4. Results of field blasting experiment

As shown in Fig. 2, inter-hole and inter-row delay times have created conditions in a way that the blast waves of the holes propagate separately in the surrounding environment. Thus, the horizontal distance of the nearest blast hole with the delay time of 527ms is considered as the source of calculating the distance to seismograph sensors. Based on this assumption, the rate of ground vibration caused by blasting operations is recorded to be 221.4m and 223.5m, respectively, using a Vibracord seismograph with two sensors and three components. In Fig. 4, placement of the seismograph sensors and in Fig. 5, the output for the vertical component of the Vibracord seismograph sensors is shown.

To assess fragmentation caused by blasting simultaneous with the loading process, numerous images were taken in a well lightened environment and from an almost perpendicular position to the fragmented pile. After the omission of low-quality images, 15 images of different locations from the fragmented pile were selected to be analyzed through the WIPFRAG image analysis software.

In Fig. 5, an example of a recorded image and the output of image analysis for the same image are shown. In Error! Reference source not found. (I), the size distribution for all analyzed images and the KCO best possible fit (with minimum MSE and maximum R) are shown in a semi-log plot. For a better illustration of the accurate fitting, especially for fine sizes, the log-log plot corresponding to the semi-log plot is shown Fig.6 (II). As seen, the average size of the fragmented material caused by blasting is 15cm and the fluctuation index is 4.5. Measurements also show that the maximum movement of the fragmented pile and the back-break caused by blasting are 25cm and 6.2cm, respectively. A schematic image of the eventual position of the pile is illustrated in Fig. 7.

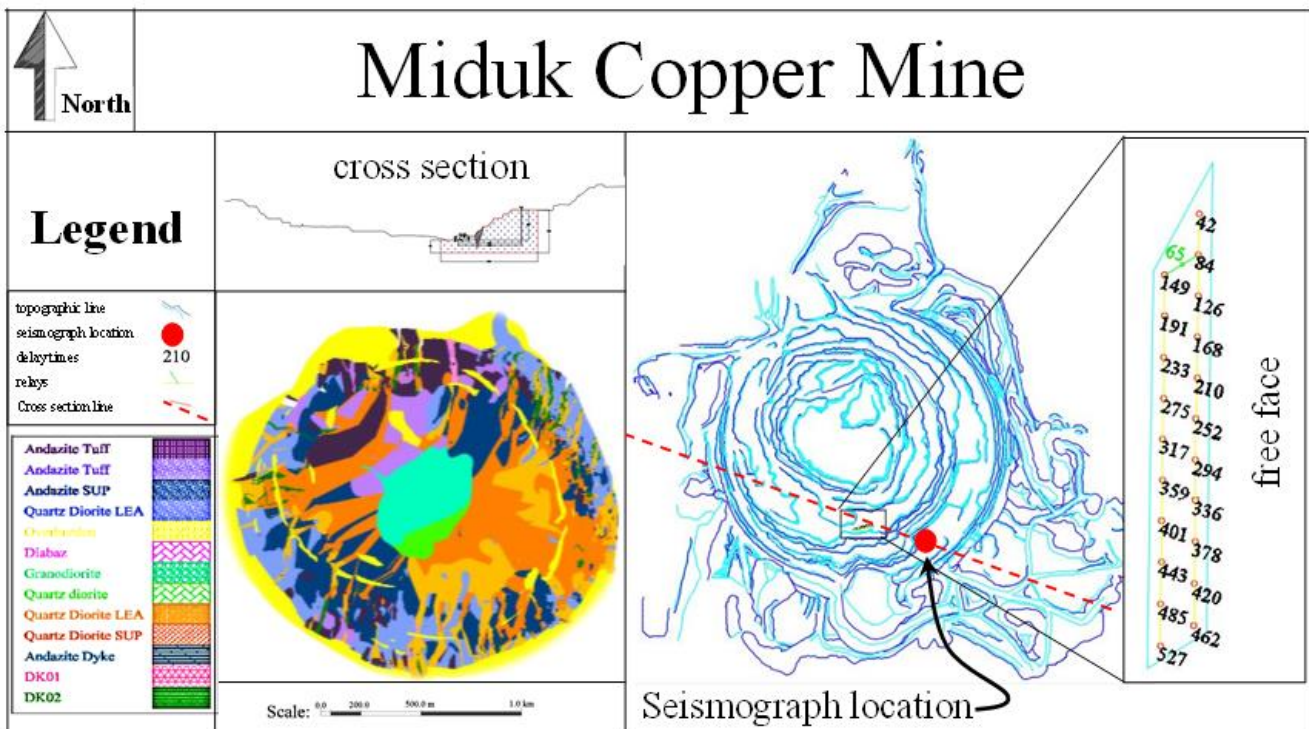


Fig. 1. Geological and topographical conditions in Miduk Copper Mine pit, Vibracord location, field blasting experiment and delay times.



Fig. 2. Field location of the blasting block and the position of the related seismographs.

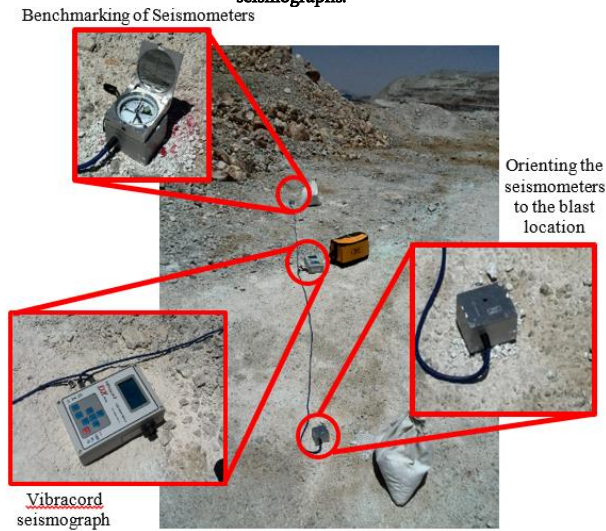


Fig. 3. Placement and leveling of the Vibracord three-component seismograph.

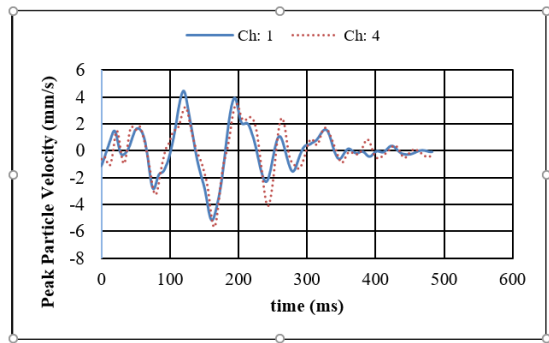


Fig. 4. Output for the vertical component of the Vibracord seismograph sensors at the distances of 223.5m (Ch: 1) and 221.4m (Ch: 4) from the blast location.

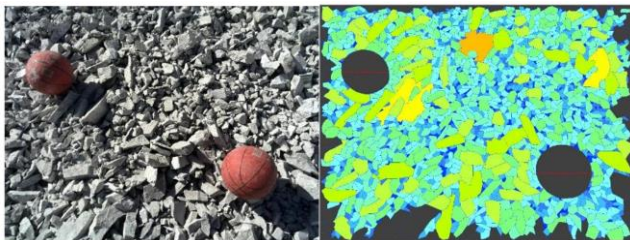


Fig. 5. An example of the photos selected for the image analysis of fragmentation caused by blasting and the WIPFRAG software output.

(I)

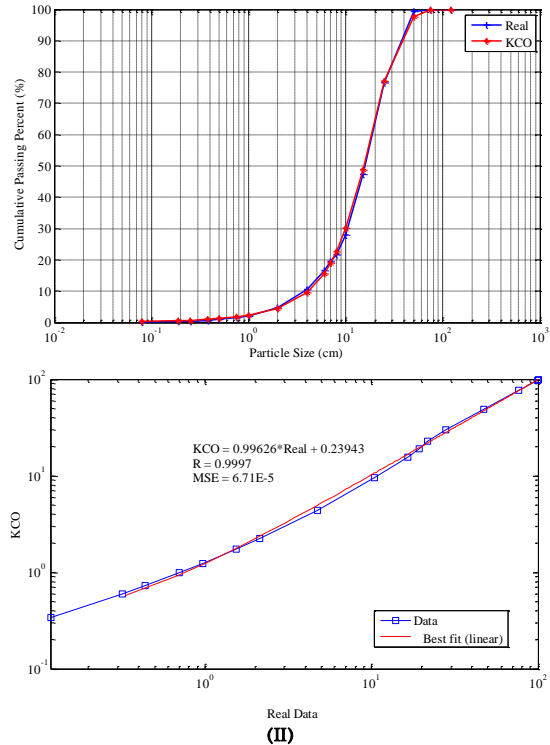


Fig. 6. The best possible fit of KCO fragmentation model to the size distribution of rock fragmentation in the Quartzite rock mass in Miduk Copper Mine: (I) semi-log and (II) log-log plots.

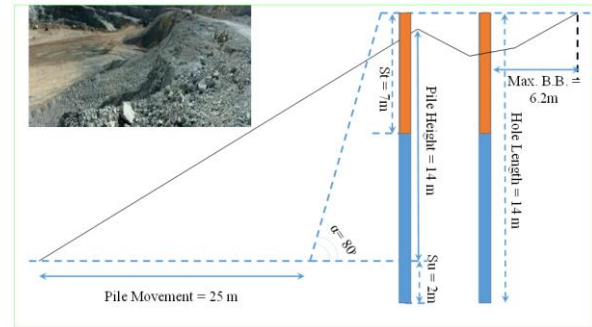


Fig. 7. A side view of the fragmented pile after blasting; according to measurements, the pile maximum horizontal movement from the slope toe is 25m and the maximum back-break is 6.2m.

### 3. Numerical modeling of blasting

In order to investigate the effect, the direction of detonation wave propagation has on the rate of ground vibration caused by blasting, the geometrical, physical and mechanical characteristics of the mine wall to the south of Miduk Copper Mine were modeled in the UDEC discrete element software. Dynamic analyses in this software were carried out in time domain assuming that there was plane stress or plane strain. To implement a dynamic model in UDEC, some stages must be experienced which are discussed in the following.

#### 3.1. Geometrical modeling and boundary conditions

To do a numerical analysis of wave propagation in the quartzite rock mass in Miduk Copper mine, a cross-section of the topographical conditions of the mine was drawn and were geometrically modeled in UDEC. The cross-sectional direction was such that it passed the seismograph and blast holes (nearest distance). Lateral and lower boundaries of the model were determined by defining boundary conditions. In order to avoid the unwanted reflection of the waves from the boundaries into the model, unlimited (viscous) boundary conditions

were applied and lateral boundaries were fixed to prevent shear displacements. The upper boundary did not have any limit and behaved as a free surface. To carry out an accurate and logical analysis of wave propagation in a numerical modeling, the size of used element ( $\Delta l$ ) had to be smaller than 0.1 to 0.125 of the length of the wave propagated in the medium [59]:

$$\Delta l \leq \left[ \frac{\lambda}{10}, \frac{\lambda}{8} \right] \quad (1)$$

where  $\lambda$  was the wavelength of the incident wave to the model. The velocity of the pressure wave could be obtained from Eq. (2) with respect to the geo-mechanical parameters of the medium [60]:

$$C_p = \sqrt{\frac{K + \frac{4G}{3}}{\rho}} \quad (2)$$

where  $\rho$  was the material density and  $K$  and  $G$  were the bulk and shear modulus, respectively. By substituting the elastic properties of the medium into the above equation, the pressure wave velocity was estimated to be 2970 m/s and the optimum size for the elements in the model was selected to be 3m. The cross-section modeled in the UDEC discrete element software, the location of the seismograph sensors, the boundary conditions, geological formations status and model dimensions are shown in Fig. 9.

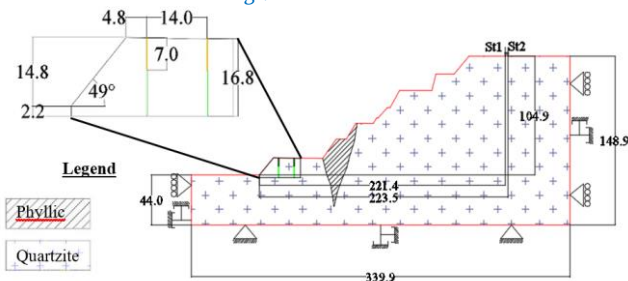


Fig. 8. Geometric modeling of the seismograph sensors' position, geometry of the blast holes, boundary conditions, geological formations status and model dimensions.

As shown in Fig. 9, the distances between the sensors and the rock were considered to be 221.4m and 223.5m, which were similar to the field conditions. In Table 1, strength properties of the Phyllic and quartzite rock masses in Miduk Copper Mine used in numerical analysis are presented.

### 3.2. Modeling dynamic loading of blasting

To model dynamic loading of the waves caused by blasting, a pressure-time pulse was used. At least three parameters of pressure-rise time, pressure-fall time and maximum blasting pressure must be known in every pressure-time pulse. According to Cook (1958) the rate of the explosives pressure is equal to the product of three quantities: particle velocity on the Chapman-Jouguet (C-J) plane, velocity of detonation and density of the explosives [61]. Thus, detonation pressure can be calculated using Eq. (3):

$$P_d = \frac{\rho_e \times VOD^2}{4} \quad (3)$$

Where  $P_d$  is the detonation pressure (Pa),  $\rho_e$  is the density of the explosives (gr/cm<sup>3</sup>) and VOD is the velocity of detonation (m/s). This is while according to Hustrulid (1999), the rate of the pressure applied to the blast hole wall equals half of the detonation pressure [2]. So, the hole pressure was calculated using Eq. (4).

$$P_h = \frac{P_d}{2} = \frac{\rho_e \times VOD^2}{8} \quad (4)$$

According to this equation, the detonation rates and the hole pressure of the ANFO (with 800 kg/m<sup>3</sup> density and 4500 m/s detonation velocity) used in the field blasting operation were 4.05GPa and 2.025GPa, respectively. The curve proposed by Yoon and Jeon (2009)

was also used in pressure-time dynamic loading whose general form is given in Eq. (5) [12].

$$P(t) = P_h \frac{e^{1-t/t_r}}{t_r} \times e^{-\left(\frac{t}{t_r}\right)} \quad (5)$$

where  $P_h$  is the hole pressure and  $t_r$  is the rise time of dynamic loading. It must be noted that in the Yoon and Jeon's proposed function, the time of pressure drop is automatically determined and its rate is approximately ten times greater than the rise time. Figure 10 shows an instance of the pressure-time pulse applied in numerical modeling. In this study, it is assumed that detonation of the explosives begins from the center of the circular cross-section and the pressure rise time is equal to the time during which the whole cross-section of the explosives column is detonated. Figure 11 also shows the assumption that detonation wave propagates inside the explosives cross-section. As shown, the time required for the pressure to rise equals to the division of the explosives radius by the velocity of detonation. Thus, pressure rise time for the detonation process was considered to be 22.57 $\mu$ s in numerical calculations. In addition, since explosives column detonation inside the blast hole was a continuous process, considering the column's length and the detonation velocity, the whole process of blasting inside the hole took place in a second fraction [2]. Thus, in numerical analysis, loading blast hole was performed step by step and the loading process (with detonation velocity of 4500m/s and charging length of 10m) took 2.3ms to finish.

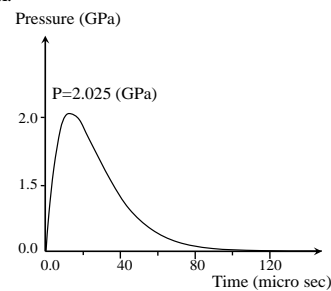


Fig. 10. Yoon and Jeon's (2009) proposed curve with the rise time of 22  $\mu$ s and the maximum pressure of 2.025GPa.

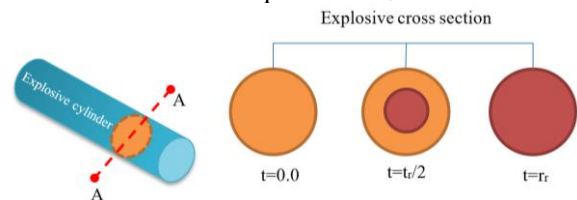


Fig. 11. Schematic image for the estimation of the rise time of the detonation for the pressure-time pulse.

### 3.3. Geometric modelling of fragmentation caused by blasting

Generally, discontinuities modeling methods are divided into three main categories. In continuous methods, plastic deformation of series of adjacent elements is considered as the development of a discontinuity. In discontinuous methods, the given area is divided into blocks in advance using fictitious cracks. Those cracks allow the blocks to slide and move over one another. However, in developed continuous methods (XFEM), the cracks growth is modeled in a unique and limited manner. Since UDEC uses discrete element logic, the best method to model fragmentation caused by blasting is to apply artificial discontinuities in such a way that statistical distribution of the blocks produced as a result of these discontinuities crossing each other is similar to the statistical distribution of fragmented materials in field blasting experiment. Fig. 12 shows the way the sets of artificial discontinuities meet, and the blocks created by them, as well as the size distribution of the blocks. As we see, size distribution of artificial blocks properly estimates the average size, and the size distribution that results from those blocks is more uniform than that of obtained in field conditions.

### 3.4. Behavioral criterion and strength properties

In fragmentation caused by blasting, the energy produced by the explosives is spent on the strengths of the rock material. For logical modeling, the strength properties of the artificial discontinuities were considered to be equal to rock material properties. Besides, to avoid unreal damping due to plastic deformation, the blocks behavioral properties were assumed to be elastic within the area of blasting block, and elasto-plastic Mohr-coulomb properties were applied for the posts outside that area.

### 3.5. Behavioral criterion and strength properties

In any natural system, part of the vibration waves energy propagate and attenuate. This phenomenon can be understood well for a system with infinite oscillation (infinite degrees of freedom) when it is exposed to a driving force (such as that of blasting). Attenuation often takes place due to energy loss through internal reactions of the materials and internal slides along the interfaces of the structural discontinuities.

In dynamic examinations carried out in the UDEC software, a two-fold semi-static-dynamic algorithm is used to take into account attenuation. Attenuation is severe in rock mass and natural soil and the Rayleigh's damping are used to attenuate a system's natural fluctuations. Rayleigh's damping equation is like a matrix in which the absorption matrix C is formed from the combination of two matrix components of M (mass component) and K (stiffness component).

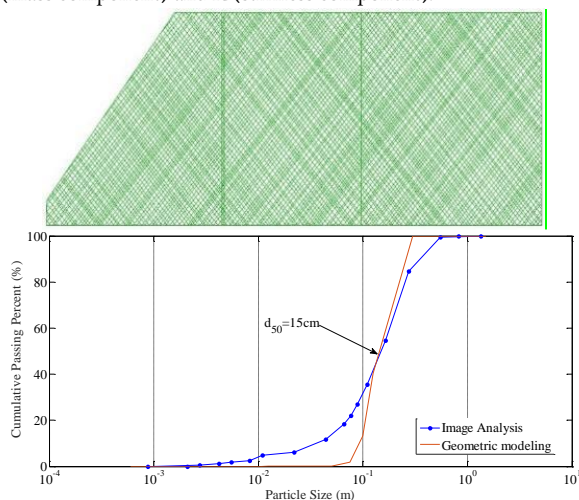


Fig. 9. Fictitious discontinuities intersections (Top) and the comparison between size distribution of the blocks created by their meeting and size distribution obtained in image analysis (Bottom).

$$C = \alpha M + \beta K \quad (6)$$

where  $\alpha$  and  $\beta$  are the mass-proportional and stiffness-proportional damping constants, respectively. In low frequencies, the mass component of damping has a higher share in total energy absorption while its stiffness component has a greater share in high frequencies.

### 3.6. Results of numerical modelling

After implementation of numerical model, completion of dynamic loading process in the blast hole and propagation of waves in the rock mass on southern wall of Miduk Copper Mine, ground vibration rate predicted in seismograph positions was recorded and compared to the measured values. In Table 2, ground vibration values calculated and recorded in field operations and numerical analyses are shown. The results of these investigations indicate that numerical analysis has acceptable accuracy and precision in estimating the rate of ground vibration caused by blasting. In Fig. 13, blast wave front propagation is shown after 0.075 seconds from the beginning of dynamic loading in the Quartzite rock mass in Miduk Copper Mine. As can be seen, the blasting wave front is crossing the non-reflective boundaries while reflection of the waves and their interference create a kind of elliptic turbulence at

the topographic level which characterize Rayleigh waves behavior. In Fig. 14, the resultant ground vibration caused by blasting is shown for seismograph number 2 (distance: 223.5m). The output of numerical software has acceptable accuracy and precision both in frequency and in estimation of maximum value for ground vibration caused by blasting. Another point is durability of the blast wave (the amount of time it continues to persist). This time is shorter in numerical analysis compared to field operations and the main reason is the effect of the third dimension of blasting (lateral holes) on the values recorded by seismograph.

Table 1. Comparing the results of numerical analysis and the values recorded by seismograph for ground vibration caused by blasting.

Row	Seismograph 2				Seismograph 1			
	radial	tangential	(PVS)	vertical	(PVS)	vertical	tangential	radial
Field operation	5.723	5.343	6.722	5.919	5.70	4.682	2.640	5.177
Numerical analysis	4.875	-	6.23	3.881	5.68	3.198	-	4.695
Percentage of error	14.9	-	7.36	34.44	0.3	31.69	-	9.3

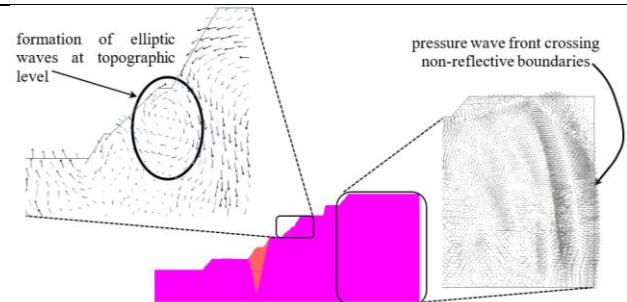


Fig. 10. Numerical modelling for formation of elliptic waves at topographic level and the wave front crossing the left hand boundary (viscous boundary condition) on the southern wall of Miduk copper mine.

## 4. Numerical analysis of the effect of detonation wave advance in the blast hole on ground vibration caused by blasting

One of the factors that can affect the blasting operation results is the position of primer in the hole. It has been experimentally confirmed that placing the primer at the bottom of the hole (aligned with the toe of the slope) can prevent the formation of a heel besides improving the degree of fragmentation. Thus, in this part of the blast hole, more force is required to overcome the strengths of the rock mass. Olofsson (1990) showed that presence of the primer at any spot in the hole, increases the velocity of detonation due to higher provocation of the explosives [62].

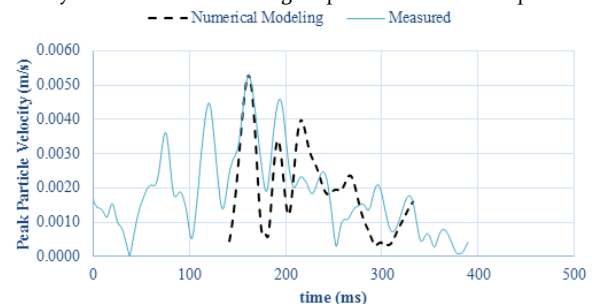


Fig. 11. Comparison between PVS of the radial and tangential components of the seismograph and that of the horizontal and vertical components predicted in numerical analysis for the 223.5m distance from the blasting location.

In this section, the effect of the primer position or the direction of detonation wave advance inside the hole on the ground vibration rate is

assessed. The effect of the primer position on formation of blast wave front is shown in Fig. 15. Due to the dependence of the blast wave front shape on the primer position, it is expected that detonation wave advance inside the blast hole affect the results of blasting operations through ground vibration. The behavior of rock mass adjacent to the blast hole during loading is a bivariate function of time and place. As shown in Fig. 15, assuming that time is constant at 1.15ms moment, the rock mass adjacent to the bottom of the hole (primer position) has been loaded from zero moment and due to the rapid propagation of the waves (longitudinal or transverse) in the rock mass, the resulting wave front has passed a distance. While blasting load is going to start at a spot in the center of the explosives column, no loading has yet taken place for a spot at the top of explosives column. Thus, the rock mass adjacent to the explosives column experiences different conditions during the loading process. Therefore, it can be stated that at near distances, blast waves propagate in conic form and the angle size of cone peak is dependent on the detonation velocity and the velocity of wave propagation in the rock mass.

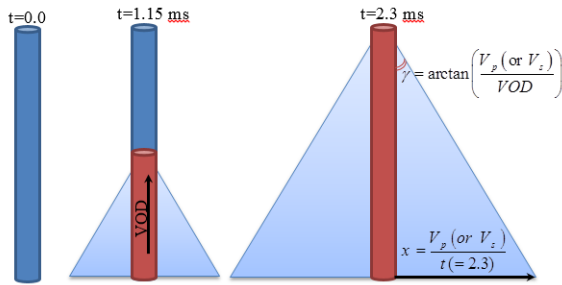


Fig. 12. Detonation wave development inside the explosives column and the propagation of the resulting waves in the rock mass adjacent to the hole.

As shown in

Fig. 13, on the opposite side of this cone, blast waves propagate in form of hemispheres and the superposition resulted from them is often destructive. To elaborate this point, it is necessary to divide the blast hole into elements with an equal length ( $dx$ ). It is assumed that the ratio of length to diameter for each of these elements is less than 6 and the resulting waves propagate in a spherical form. Therefore, the time required to blast each of these elements can be calculated by Eq. (7).

$$t = \frac{dx}{VOD} \quad (7)$$

where  $VOD$  is detonation velocity and  $t$  is the time an element with the length of  $dx$  detonates. Thus, the required time for each element to detonate is an integer obtained from the multiplication of element number by  $t$ . However, if the source of calculations is bottom of the hole and the waves created by detonation of each element are assumed to be spherical, the second element detonates at  $2 \times t$  moment and the blast wave of the first element passes through a distance calculated by Eq. (8).

$$r_1 = Vt = V_p \times \frac{dx}{VOD} - \frac{dx}{2} \quad (8)$$

Thus, at the  $3 \times t$  moment, the third element detonates and at this moment, the spherical waves caused by the first and second elements have passed different distances. The distance passed by the spherical waves of the first and the second elements are  $r_1 = \frac{2 \times V_p \times dx}{VOD} - \frac{dx}{2}$  and

$r_1' = \frac{V_p \times dx}{VOD} - \frac{3 \times dx}{2}$ , respectively. So, the distance between the two consecutive spherical wave fronts caused by the blasting is calculated by Eq. (9).

$$(9)$$

$$\begin{aligned} r_2 - r_1' &= \left[ \frac{2 \times V_p \times dx}{VOD} - \frac{dx}{2} \right] - \left[ \frac{V_p \times dx}{VOD} - \frac{3 \times dx}{2} \right] \\ &= \frac{V_p \times dx}{VOD} + dx \\ &= dx \left[ \frac{V_p}{VOD} + 1 \right] > 0 \end{aligned}$$

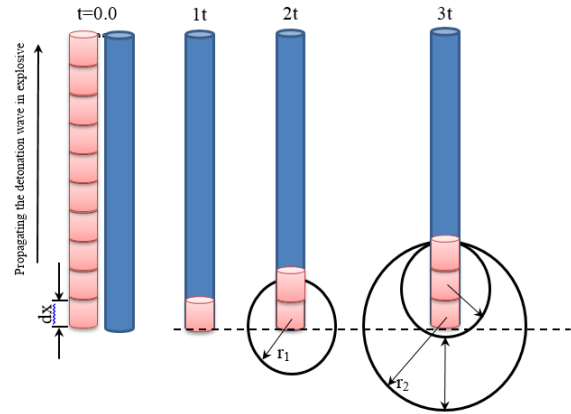


Fig. 13. Semi-spherical waves propagated in the opposite direction of detonation wave advance and impossibility of constructive superposition among them.

As it can be seen, the difference in phase of the spherical waves caused by adjacent elements is always greater than zero and they do not have a constructive superposition. Therefore, superposition of the wave hemisphere in the opposite direction of the detonation wave advance in the blast hole is destructive and causes less ground vibration.

On this basis and in completely similar geometric and geo-mechanical conditions, a two-dimensional cross-section of the blasting block with one blast hole was modeled in the UDEC discrete element software for primer status at the bottom and at the top of the hole. Since the blast conical wave front has different directions for the two statuses, it is expected that ground vibrations caused by blasting at different directions yield different values. According to the results of numerical analysis, the rate of ground vibration caused by blasting, increases when the primer position changes from the bottom of the hole to its top. In Fig.17, changes in the values of maximum particle velocity caused by blasting (the PVS of horizontal and vertical components) at the distances of 8m, 12m, 16m and 20m are shown for downward blasting status (where the primer is placed at the top of the hole) and upward status (where the primer is at the bottom of the hole). As seen, in downward blasting, due to the direction of the conical wave front's top towards the ground, the energy of the waves is concentrated and transferred to the ground to create a higher rate of ground vibration.

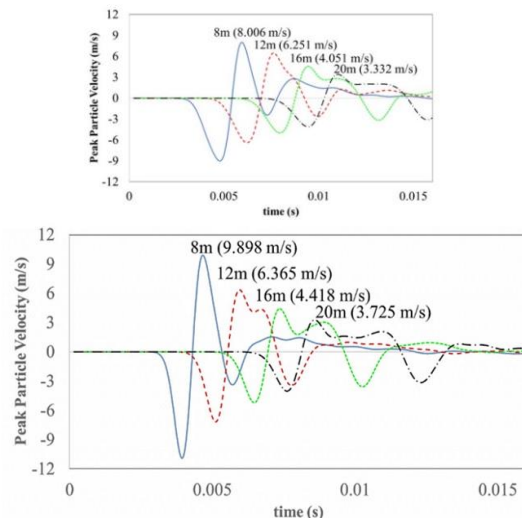


Fig. 14. Output for the PVS of vertical and horizontal components of particle

### velocity in the numerical modeling of upward (Top) and downward (Bottom) blasting.

## 5. Conclusion

In this study, the effects of primer location on ground vibration caused by blasting operation were investigated using numerical modeling. To validate the results of numerical analysis, a field experiment was conducted in the Quartzite rock mass in Miduk Copper Mine and its results including ground vibration, fly-rock, back-break, fragmentation and movement of the fragmented pile were recorded. Using UDEC discrete element software, a two-dimensional cross-section of the blasting block location was drawn and its geological and geometrical conditions were modeled. In numerical analysis, dynamic loading conditions of the blast were modeled through sequential shock waves in the blast hole and propagation of the blast waves in the Quartzite rock mass was investigated. The results of numerical analysis showed acceptable accuracy and precision of the UDEC software in estimating ground vibration caused by blasting. Having tested the accuracy of the data, a blasting block was modeled and the effect of detonation wave front advance on the superposition of blast waves was analyzed. Due to the constructive superposition of blast waves in line with the advancement of detonation wave inside the blast hole, the wave front propagated in the adjacent rock mass in the form of a cone and the energy content was higher at the cone apex. This phenomenon was modeled for conditions where the primer is placed at the bottom or top of the blast hole. Results of numerical analysis confirmed that the direction of detonation wave propagation affects the amount of ground vibration caused by blasting. According to the results of analytical calculations and numerical analysis, when the primer is at the bottom of the blast hole, the orientation of blasting cone waves is towards the upper part of the blast hole and ground vibration in this condition is lower than the other. Placing the primer in the center of the column of explosives creates waves with complex super-positions since two cone wave fronts are formed on two sides of the blast hole and interfere with destructive waves hemisphere but it is expected that the resulting ground vibration to be the average of two above-mentioned states.

## Acknowledgements

This study was supported by Iranian Copper Industries National Company, and the authors would like to thank the managerial service affairs (research center) in Miduk Copper Mine them for providing the facilities required to conduct the study.

## References

- [1] Jimeno CL, Jimeno EL, Carcedo FJA. *Drilling and Blasting of Rocks*. Rotterdam, Netherlands: AA Balkema; 1995.
- [2] Hustrulid W. *Blasting Principles for Open Pit Mining*: AA Balkema, Rotterdam, Netherlands; 1999.
- [3] Cooper PW. *Explosives Engineering*. Canada: Wiley-VCH, Inc; 1997.
- [4] Udy LL, Lownds CM. The Partition of Energy in Blasting with non-ideal Explosives. *Proceedings of the 3rd International Symposium on Rock Fragmentation by Blasting, Fragblast 3*. Australia, Brisbane: CRC Press: Taylor and Francies Group; 1990. p. 37-43.
- [5] Wyllie DC, Mah C. *Rock slope engineering*: CRC Press; 2004.
- [6] Singh T, Singh V. An intelligent approach to prediction and control ground vibration in mines. *Geotech Geo-Eng*. 2005;23:249-62.
- [7] Grady D, Kipp M. Geometric statistics and dynamic fragmentation. *J Appl Phys*. 1985;58:1210-22.
- [8] Bhandari S. *Engineering Rock Blasting Operations*. Balkemma/Rotterdam1997.
- [9] Chen S, Zhao J, Zhou Y. UDEC modeling of a field explosion test. In: *Proceedings of the 7th International Symposium on Rock Fragmentation by Blasting (Fragblast-7)*: CRC Press; 2000. p. 149-63.
- [10] You-jun N, Jun Y. Numerical Simulation of the Blasting Process in Bedded and Jointed Rock Mass with 2D-DDA Method. *Proceedings of the 8th International Symposium on Rock Fragmentation by Blasting, Fragblast 8*. Santiago, Chile: CRC Press: Taylor and Francis Group; 2006. p. 119-23.
- [11] Kim D, Noh S, Lee S, Park B, Jeon S. Development of a new center-cut method: SAV-cut (Stage Advance V-cut). *Underground Space*. In: Barták, Hrdina, Romancov, Zlámál, editors. *The 4th Dimension of Metropolises*. London: Taylor & Francis Group; 2007. p. 493-9.
- [12] Yoon J, Jeon S. Use of a Modified Particle-Based Method in Simulating Blast-Induced Rock Fracture. *Proceedings of the 9th International Symposium on Rock Fragmentation by Blasting, Fragblast 9*. Granada, Spain: CRC Press: Taylor & Francis Group; 2010. p. 371-80.
- [13] Furtney JK, Sellers EJ, Onederra I. Simple models for the complex process of rock blasting In: Sinha S, editor. *Proceedings of the 10th International Symposium on Rock Fragmentation by Blasting, Fragblast 10*. New Dehli, India: CRC Press: Taylor & Francis Group; 2013. p. 275-82.
- [14] Sharpe JA. The production of elastic waves by explosion pressures. I. Theory and empirical field observations. *Geophysics*. 1942;7:144-54.
- [15] Favreau R. Generation of strain waves in rock by an explosion in a spherical cavity. *Journal of Geophysical Research*. 1969;74:4267-80.
- [16] Miklowitz J. *The Theory of Elastic Waves and Waveguides*. New York: North-Holland Publishing Company; 1990.
- [17] Pusch R, Stanfors R. Zone of Disturbance around Blasted Tunnels at Depth. *International Journal of Rock Mechanics and Mining Science and Geomechanics Abstracts*. 1992;29:447-56.
- [18] Paine AS, Please CP. Improved model of fracture Propagation by Gas during Rock Blasting-Some Analytical Results. *International Journal of Rock Mechanics and Mining Science*. 1994;699-706.
- [19] Yu B, Liu D, Qiao H, Wang S. Experimental Study of granite's constitutive relation under blasting loads. *Journal of China University of Mining and Technology*. 1999;28:552-5.
- [20] Esen S, Onederra I, Bilgin H. Modelling the size of the crushed zone around a blasthole. *Int J Rock Mech Min Sci*. 2003;40:485-95.
- [21] Hongtao X, Wenbo L, Chaungbing Z. Effect of Dynamic Unloading during the Process of Rock Fragmentation by Blasting. *International Proceedings of Rock Fragmentation by Blasting, Fragblast-8*. Santiago-chile2006. p. 175-81.
- [22] Müller B, Hausmann J, Niedzwiedz H. Control of rock fragmentation and muck pile geometry during production blasts (environmentally friendly blasting technique). *Proceedings of 9th Rock Fragmentation by Blasting Symposium, Fragblast 9*. Granada, Spain: CRC Press: Taylor & Francis Group; 2010. p. 277-86.
- [23] Stojadinović S, Pantović R, Žikić M. Prediction of flyrock trajectories for forensic applications using ballistic flight equations. *International Journal of Rock Mechanics and Mining Sciences*. 2011;48:1086-94.
- [24] Ghasemi E, Sari M, Ataei M. Development of an empirical model for predicting the effects of controllable blasting parameters on flyrock distance in surface mines. *International Journal of Rock Mechanics & Mining Sciences*. 2012;163-70.
- [25] Stojadinović S, Lilić N, Pantović R, Žikić M, Denić M, Čokorilo V, et al. A new model for determining flyrock drag coefficient. *International Journal of Rock Mechanics and Mining Sciences*. 2013;62:68-73.
- [26] Hustrulid WA, Johnson JC. A Gas Pressure-based Drift Round Blast Design Methodology. In: Schunnesson H, Nordlund E, editors. *5th International Conference & Exhibition on Mass Mining*. Sweden, Lulea: Lulea University of Technology; 2008. p. 657-69.
- [27] Iverson SR, Hustrulid WA, Johnson JC, Akbarzadeh Y. The Extent of Blast Damage from a Fully Coupled Explosive Charge. In:

- Sanchidrián J, editor. Proceedings of the 9th International Symposium on Rock Fragmentation by Blasting, Fragblast 9. Granada, Spain: CRC Press: Taylor and Francis Group; 2010. p. 459-68.
- [28] Gheibie S, Aghababaei H, Hoseinie S, Pourrahimian Y. Modified Kuz—Ram fragmentation model and its use at the Sungun Copper Mine. *Int J Rock Mech Min Sci.* 2009;46:967-73.
- [29] Harries GH. The Calculation of Heave and Muck-Pile Profile. Proceedings of the 2nd International Symposium on Rock Fragmentation by Blasting, Fragblast 2. Keystone, Colorado: CRC Press: Taylor and Francis Group; 1987. p. 248-56.
- [30] Kirby IJ, Harries GH, Tidman JP. ICI's Computer Blasting Model SABREX - Blast Principles and Capabilities. Proceedings of the 13th Conference on Explosives and Blasting Technique. Miami, Florida: ISEE - International Society of Explosives Engineers; 1987. p. 1-6.
- [31] Yang RL, Kavetsky A. A Three Dimensional Kinematic Model of Muckpile Formation in Bench Blasting. Proceedings, AusIMM, Explosives in Mining Workshop. Melbourne, Australia 1988. p. 45-9.
- [32] Yang RL, Kavetsky A. A Three Dimensional Model of muckpile formation and Grade Boundary Movement Open Pit Blasting. *International Journal of Mining and Geological Engineering.* 1990:13-43.
- [33] Preece DS, Knudsen SD. Coupled Rock Motion and Gas Flow Modeling in Blasting. 8th Annual Symposium on Explosives and Blasting Research: ISEE, International Society of Explosives Engineers; 1992.
- [34] Preece D. A numerical study of bench blast row delay timing and its influence on percent cast. Sandia National Labs., Albuquerque, NM (United States); 1992.
- [35] Chung S, McGill M, Preece DS. Computer cast blast modelling. International Society of Explosives Engineers, Cleveland, OH (United States); 1994.
- [36] Chen SG, Zhao J. A Study of UDEC Modelling for Blast Wave Propagation in Jointed Rock Masses. *Int J Rock Mech Min Sci.* 1998;35:93-9.
- [37] Preece D, Chung S. Modeling Coal Seam Damage in Cast Blasting. In Proceedings of the Annual Conference on Explosives and Blasting Technique: International Society of Explosives Engineering; 1999. p. 233-40.
- [38] Mortazavi A, Katsabanis P. Modelling Burden Size and Strata Dip effects on the Surface Blasting Process. *Int J Rock Mech Min Sci.* 2001;38:481-98.
- [39] Shi G-H. Discontinuous deformation analysis: a new numerical model for the statics and dynamics of deformable block structures. *Engineering computations.* 1992;9:157-68.
- [40] Firth IR, Taylor DL. Bench Blast Modeling Using Numerical Simulation and Mine Planning Software. SME Annual Meeting, Denver, Colorado: SME; 2001.
- [41] Fan S, Jiao Y, Zhao J. On modelling of incident boundary for wave propagation in jointed rock masses using discrete element method. *Computers and Geotechnics.* 2004;31:57-66.
- [42] Ning Y, Yang J, Ma G, Chen P. Modelling rock blasting considering explosion gas penetration using discontinuous deformation analysis. *Rock mechanics and rock engineering.* 2011;44:483-90.
- [43] Aliabadian Z, Sharafisafa M, Mortazavi A, Maarefvand P. Wave and fracture propagation in continuum and faulted rock masses: distinct element modeling. *Arabian Journal of Geosciences.* 2014;7:5021-35.
- [44] Sharafisafa M, Aliabadian Z, Alizadeh R, Mortazavi A. Distinct element modelling of fracture plan control in continuum and jointed rock mass in presplitting method of surface mining. *International Journal of Mining Science and Technology.* 2014;24:871-81.
- [45] Yan P, Zhou W, Lu W, Chen M, Zhou C. Simulation of bench blasting considering fragmentation size distribution. *International Journal of Impact Engineering.* 2016;90:132-45.
- [46] Bahadori M, Bakhshandeh Amnieh H, Khajezadeh A. A new geometrical-statistical algorithm for predicting two-dimensional distribution of rock fragments caused by blasting. *International Journal of Rock Mechanics and Mining Sciences.* 2016;86:55-64.
- [47] Starfield AM, Pugliese JM. Compression waves generated in rock by cylindrical explosive charges: A comparison between a computer model and field measurements. *International Journal of Rock Mechanics and Mining Science & Geomechanics Abstracts.* 1974;5:65-77.
- [48] Preece DS, Thorne BJ. A study of detonation timing and fragmentation using 3D finite element techniques and damage constitutive model. Proceedings of the 5th International Symposium on Rock Fragmentation by Blasting, Fragblast 5. Montreal, Quebec, Canada: CRC Press: Taylor and Francis Group; 1996. p. 147-56.
- [49] Liu L, Katsabanis P. A Numerical Study of the Effects of Accurate Timing on Rock Fragmentation. *Int J Rock Mech Min Sci.* 1997 34:817-35.
- [50] Wenxue G, Yuntong L, Hailong Y. Dynamic Damage Model of Brittle Rock and Its Application. In: Xuguang W, editor. Proceedings of the 6th International Symposium on Rock Fragmentation by Blasting, Fragblast 6. Beijing, China: CRC Press: Taylor & Francis Group; 2002. p. 128-32.
- [51] Cho SH, Nishi M, Yamamoto M, Kaneko K. Fragment Size Distribution in Blasting. *Materials Transactions.* 2003;44:951-6.
- [52] Jha AK, Deb D, Jha NC. Impact Assessment of Surface Mine Blasting on Adjacent Underground Mine Structures Using Field Measurements and Numerical Techniques. In: Sanchidrián J, editor. Proceedings of the 9th International Symposium on Rock Fragmentation by Blasting, Fragblast 9. Granada, Spain: CRC Press: Taylor and Francis Group; 2010. p. 571-7.
- [53] Sazid M, Singh TN. Two-dimensional dynamic finite element simulation of rock blasting. *Arabian Journal of Geosciences.* 2012;6:3703-8.
- [54] Jing L, Hudson J. Numerical methods in rock mechanics. *Int J Rock Mech Min Sci.* 2002;39:409-27.
- [55] Furtney J, Cundall P, Chitombo G. Developments in numerical modeling of blast induced rock fragmentation: Updates from the HSBM project. Rock Fragmentation by Blasting-Proceedings of the 9th International Symposium on Rock Fragmentation by Blasting, FRAGBLAST 9: CRC Press; 2009. p. 335-42.
- [56] Onederra I, Chitombo G, Cundall P, Furtney J. Towards a complete validation of the lattice scheme in the Hybrid Stress Blasting Model (HSBM). In: Sanchidrián J, editor. Proceedings of the 9th International Symposium on Rock Fragmentation by Blasting, Fragblast 9. Granada, Spain: CRC Press: Taylor & Francis Group; 2010. p. 343-51.
- [57] Sellers E, Kotze M, Dipenaar L, Ruest M. Large scale concrete cube blasts for the HSBM model. In: Sanchidrián J, editor. Proceedings of the 9th International Symposium on Rock Fragmentation by Blasting, fragblast 9. Granada, Spain: CRC Press: Taylor & Francis Group; 2010. p. 389-98.
- [58] Sellers E, Furtney J, Onederra I, Chitombo G. Improved understanding of explosive-rock interactions using the hybrid stress blasting model. *Journal of the Southern African Institute of Mining and Metallurgy.* 2012;112:721-8.
- [59] Kuhlemeyer RL, Lysmer J. Finite element method accuracy for wave propagation problems. *Journal of Soil Mechanics & Foundations Div.* 1973;99.
- [60] UDEC. Itasca C. G; UDEC 4 Manual. Minneapolis 2004.
- [61] Cook MA. The science of high explosives: RE Krieger Pub. Co.; 1958.
- [62] Olofsson SO. Applied explosives technology for construction and mining: Applex; 1990.